Mendeleev Communications

Mendeleev Commun., 2025, **35**, 228–230

Selective hydrogenation of nitrobenzene to aniline over $LaNiO_3$

Olga P. Tkachenko,*[a] Elena V. Shuvalova,[a] Petr V. Zemlianskii,[a] Nikolay A. Davshan[a] and Leonid M. Kustov[a,b]

[a] *N. D. Zelinsky Institute of Organic Chemistry, Russian Academy of Sciences, 119991 Moscow, Russian Federation. E-mail: ot@ioc.ac.ru*

[b] *Department of Chemistry, M. V. Lomonosov Moscow State University, 119991 Moscow, Russian Federation*

DOI: 10.71267/mencom.7599

Perovskite $LaNiO_3$ prepared by the glycine–nitrate method was studied by XPS, XRD and SEM-EDS. This substance was tested as the catalyst in the hydrogenation of nitrobenzene to aniline in ethanol (150 °C, 1.5 MPa H_2). The selectivity for aniline was 95.6% with a conversion of 98.7%. According to XPS data, La and Ni do not change their electronic state in the course of the reaction.

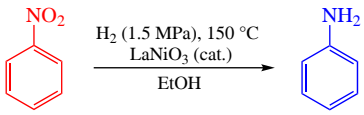

Keywords: $LaNiO_3$, hydrogenation, nitrobenzene, aniline, XPS, XRD, SEM-EDS.

The amino group of anilines makes them an important intermediate for the production of drugs, dyes, rubber, explosives, fertilizers, pesticides and herbicides. Currently, almost all aniline in the world is produced by the catalytic reduction of nitrobenzene with hydrogen. To obtain anilines by gas-phase hydrogenation of nitrobenzenes, Ni- or Cu-containing catalysts are used.[1] In liquid-phase hydrogenation, in addition to these metals, Pd-, Ru-, Au- In- and Rh-containing catalysts on various supports are also used.[2–16] Perovskite-type transition metal oxides are good alternative to noble metal catalysts due to high activity, thermal stability, ease of preparation and, as a result, low cost. They were used for CO, CO_2, dinitrobenzene, guaiacol, glycerol and xylose hydrogenation.

The present work was aimed to inspect the catalytic behavior of $LaNiO_3$ perovskite in the direct hydrogenation of nitrobenzene with molecular hydrogen. Perovskite $LaNiO_3$ containing highly dispersed nickel cations was tested for the first time in this reaction. Perovskite $LaNiO_3$ was prepared by the glycine–nitrate method (details on the preparation with texture and the XRD characterizations of the obtained sample as well as the hydrogenation experiment are given in Online Supplementary Materials).

Both samples, before and after catalysis, were studied by the electron microscopy and X-ray photoelectron spectroscopy methods. Survey XP spectra of $LaNiO_3$ before and after catalysis contain photoelectron lines of carbon, oxygen, lanthanum, and nickel, and weak Auger electron lines of La MNN. The high-resolution photoelectron spectra of C 1s and O 1s electrons are shown in Figures 1 and 2.

The XP spectra of the fresh and waist samples for La and Ni atoms (Figure 3) show that La $3d_{3/2}$ and Ni $2p_{3/2}$ photoelectron lines overlap. The energy position of La $3d_{5/2}$, Ni $2p_{3/2}$ and O 1s electrons, the full width at half maximum of the lines, and the elemental composition of the surface are presented in Table 1. Since the photoelectron lines of La $3d_{3/2}$ and Ni $2p_{3/2}$ overlap, non-overlapping lines La $3d_{5/2}$ and Ni $2p_{1/2}$ were used for quantitative assessment.

According to Table 1, it is clear that La and Ni in the surface layers of both samples exist in the oxidation state of La^{3+} and Ni^{2+}.[17–19] The electron density on La^{3+} cations does not change during the catalysis process, but the line becomes narrower. The electron density on nickel cations Ni^{2+} in the sample after

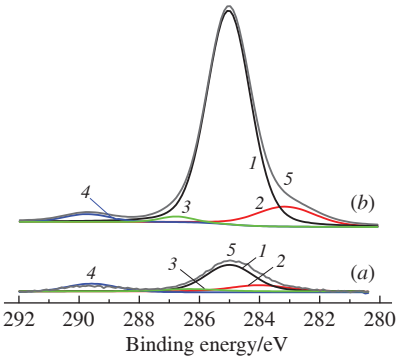

Figure 1 XP C 1s spectra: (*a*) before and (*b*) after catalysis. C 1s curves correspond to: alkanes (binding energy E_b = 285.0 eV, curves *1*), carbonaceous deposits (E_b = 283.1–284 eV, curves *2*); alcohols and ethers (E_b = 286.3–286.7 eV, curves *3*), carbonates or esters (E_b = 289.6–289.7 eV, curves *4*); curves *5* represent the real XP spectrum, *i.e.* the superposition of deconvoluted curves *1*–*4*.

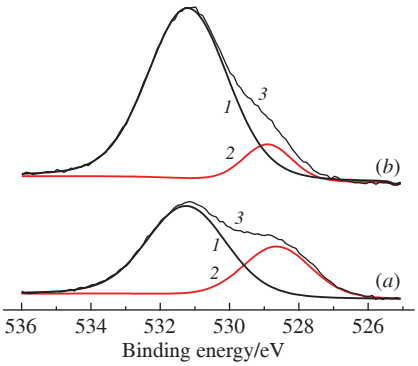

Figure 2 XP O 1s spectra: (*a*) before and (*b*) after catalysis. O 1s curves are assigned to: OH^- (E_b = 531.2 eV, curves *1*) and to O^{2-} species (E_b = 528.6–528.9 eV, curves *2*); curves *3* represent the XP spectrum, *i.e.* the superposition of deconvoluted curves *1*, *2*.

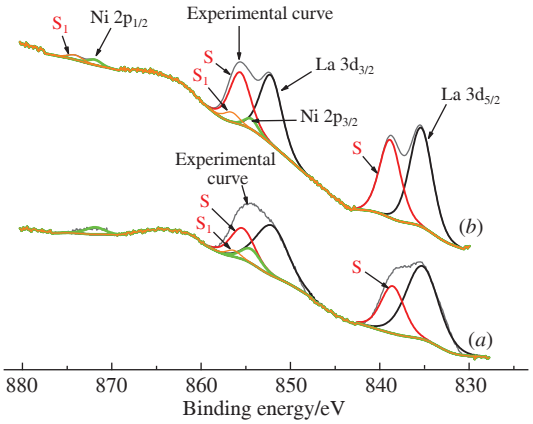

Figure 3 XP La 3d and Ni 2p spectra (*a*) before and (*b*) after catalysis. S stands for shake-up satellite of La 3d lines, S_1 stands for shake-up satellite of Ni 2p lines.

Table 1 XPS data of the $LaNiO_3$–glycine catalyst.

Sample	Binding energy/eV (FWHM/eV)			Atomic ratio	
	La $3d_{5/2}$	Ni $2p_{3/2}$	O 1s(O^{2-})	La/Ni	O/La
Before catalysis	835.1 (4.3)	854.4 (2.5)	528.6 (2.3)	9.9	5.7
After catalysis	835.1 (3.0)	854.3 (1.7)	528.9 (1.7)	16.4	14.7

catalysis decreases slightly, and the line also becomes narrower. The electron density on the O^{2-} oxygen anions increases slightly during the catalysis process, and the line also becomes narrower. The La/Ni atomic ratio on the surface of the sample before catalysis is much higher than stoichiometric, and after catalysis it increases significantly (almost 2 times). The calculation of the Ni content according to XPS data was 7.02 wt% before catalysis and 13.14 wt% after catalysis. The average weight content of Ni is 10 wt%. This value was used in TOF calculations. Literature data from the surface-sensitive XPS method indicate that the surface of $LaNiO_{3-x}$ perovskite samples prepared by chemical synthesis is enriched with lanthanum and oxygen.[20–23]

Both fresh and waist samples of the catalyst were additionally investigated by SEM micrographs as well as electron diffraction study (EDS) (see Online Supplementary Materials, Figures S6, S7 and Table S1). The EDS data show that the La/Ni ratio in both samples remains practically the same (close to 1), while those from XPS demonstrated a significant growth of the La/Ni ratio in the course of the aniline hydrogenation (see Table 1). This significant difference may be accounted for the depth of the analyzed layer (20–30 Å in XPS *vs.* 1 μm in EDS). X-ray diffraction study (XDS) confirmed the crystal nature of perovskite $LaNiO_3$ (see Online Supplementary Materials, Figure S8 and comments therein).

The experiments on hydrogenation of nitrobenzene (1.5 MPa H_2, 150 °C, EtOH) show that after 7 h it is almost completely hydrogenated to the target aniline (Table 2 and Figure S9). In the course of the hydrogenation, intermediates such as azobenzene, azoxybenzene and hydrazobenzene, should be formed; however, they were not detected during the GC analysis.[5]

Table 2 Hydrogenation of nitrobenzene into aniline over $LaNiO_3$.

t/h	Conversion (%)	Selectivity (%)	TOF[a]/h^{-1}
1	13.2	15.4	0.208
2	34.1	36.9	0.644
3	48.2	46.3	0.761
4	50.1	62.5	0.802
6	92.6	91.1	1.438
7	98.7	95.6	1.381

[a]The turnover frequency was expressed taking into account the selectivity normalized to the Ni content for the specified time.

Comparison of our results with the literature data (see Online Supplementary Materials, Table S2) shows that the selectivity toward aniline was in general at a level of 80–100%. With one exception of the gas-phase process,[1] the reaction was usually performed in ethanol solution at moderate temperatures of 35–150 °C. Some catalysts similar to Raney nickel and containing much metallic nickel provided high conversions,[6,14] while this parameter with a catalyst containing 36 wt% of nickel was low.[3] Another catalyst with a low nickel content was characterized by low selectivity although with full conversion.[13] The catalyst 10%Ni/C(mineral)[9] and the catalyst studied in the present work are comparable in terms of the nickel content and both provide high conversion and selectivity. However, the working temperature of our sample is high enough (at temperatures lower than 150 °C, the reaction is slow), which may be a challenge for further improvement of such a novel lanthanum-containing hydrogenation catalyst.

In summary, the catalytic hydrogenation of nitrobenzene into aniline in the presence of $LaNiO_3$ with the perovskite structure provides 95.6% selectivity with a conversion of 98.7%. According to the EDS data, the atomic ratio La/Ni did not change during the reaction. At the same time, in the surface layers accessible to XPS (20–30 Å), an increase in this ratio was detected. According to the XPS data, the electronic state of both components did not change. It was shown that Ni^{2+} stabilized in the $LaNiO_3$ perovskite structure demonstrates good efficiency compared to Ni^0 supported catalysts.

This work was financially supported by the Ministry of Science and Higher Education of the Russian Federation (project 075-15-2023-585). Electron microscopy characterization was performed in the Department of Structural Studies of Zelinsky Institute of Organic Chemistry, Moscow.

Online Supplementary Materials

Supplementary data associated with this article can be found in the online version at doi: 10.71267/mencom.7599.

References

1 Y. Jiang, X. Li, Z. Qin and H. Ji, *Chin. J. Chem. Eng.*, 2016, **24**, 1195; https://doi.org/10.1016/j.cjche.2016.04.030.
2 O. Verho, K. P. J. Gustafson, A. Nagendiran, C.-W. Tai and J.-E. Bäckvall, *ChemCatChem*, 2014, **6**, 3153; https://doi.org/10.1002/cctc.201402488.
3 X. Meng, H. Cheng, Y. Akiyama, Y. Hao, W. Qiao, Y. Yu, F. Zhao, S.-I. Fujita and M. Arai, *J. Catal.*, 2009, **264**, 1; https://doi.org/10.1016/j.jcat.2009.03.008.
4 M. Turáková, T. Salmi, K. Eränen, J. Wärnå, D. Yu. Murzin and M. Králik, *Appl. Catal., A*, 2015, **499**, 66; https://doi.org/10.1016/j.apcata.2015.04.002.
5 E. A. Gelder, S. D. Jackson and C. M. Lok, *Chem. Commun.*, 2005, 522; https://doi.org/10.1039/b411603h.
6 X. Zhou, H. Zhao, S. Liu, D. Ye, R. Qu, C. Zheng and X. Gao, *Appl. Surf. Sci.*, 2020, **525**, 146382; https://doi.org/10.1016/j.apsusc.2020.146382.
7 V. Yu. Doluda, G. N. Demidenko, M. G. Sulman, N. V. Lakina, V. G. Matveeva and E. M. Sulman, *Izv. Vyssh. Uchebn. Zaved., Khim. Khim. Tekhnol.*, 2013, **56** (6), 62 (in Russian); https://ctj-isuct.ru/public/journals/2/2013/v56_n06_2013_full.pdf.
8 O. Ya. Polotnyuk, *Kataliz v promyshlennosti*, 2013, no. 4, 77 (in Russian); https://www.catalysis-kalvis.ru/jour/article/view/116/113.
9 E. N. Terekhova, O. B. Belskaya, R. R. Izmaylov, M. V. Trenikhin and V. A. Likholobov, *Catalysts*, 2023, **3**, 82; https://doi.org/10.3390/catal13010082.
10 A. Filatova, V. Matveeva, E. Shumanskaya and L. Mushinskii, *Byull. nauki i praktiki*, 2018, **4** (12), 89 (in Russian); https://doi.org/10.5281/zenodo.2254348.
11 S. Gómez, C. Torres, J. L. G. Fierro, C. R. Apestegula and P. Reyes, *J. Chil. Chem. Soc.*, 2012, **57**, 1194; https://doi.org/10.4067/S0717-97072012000200029.

12 A. V. Rassolov, G. A. Ivanov, G. O. Bragina, G. N. Baeva, N. S. Smirnova, A. V. Kazakov, N. Ya. Usachev and A. Yu. Stakheev, *Kinet. Catal.*, 2021, **62**, 641; https://doi.org/10.1134/s0023158421050062.
13 B. Klausfelder and R. Kempe, *Z. Anorg. Allg. Chem*., 2023, **649**, e202300071; https://doi.org/10.1002/zaac.202300071.
14 A. Das, K. M. Hansda, A. Mahato, P. Singh and N. Mahata, *J. Indian Chem. Soc*., 2020, **97**, 2948; https://doi.org/10.5281/zenodo.5654751.
15 E. V. Shuvalova and O. A. Kirichenko, *Mendeleev Commun*., 2024, **34**, 587; https://doi.org/10.1016/j.mencom.2024.06.039.
16 E. G. Chepaikin, S. I. Pomogailo, O. P. Tkachenko, E. V. Shuvalova, L. M. Kustov, V. N. Borshch, E. I. Knerel'man and D. A. Pomogailo, *Russ. J. Phys. Chem. A*, 2024, **98**, 1233; https://doi.org/10.1134/S003602442470016X.
17 C. D. Wagner, W. M. Riggs, L. E. Davis, J. F. Moulder and G. E. Muilenberg, *Handbook of X-ray Photoelectron Spectroscopy*, Perkin-Elmer Corp., Eden Prairie, MN, 1979; https://doi.org/10.1002/sia.740030412.
18 A. V. Naumkin, A. Kraut-Vass, S. W. Gaarenstroom, C. J. Powell and A. Y. Lee, *NIST X-ray Photoelectron Spectroscopy Database*, 2023; https://doi.org/10.18434/T4T88K.
19 C. D. Wagner, in *Practical Surface*, *Analysis Auger and X-ray Photoelectron Spectroscopy*, 2nd edn., eds. D. Briggs and M. Seah, Wiley, Chichester, 1990, vol. 1, pp. 595–634.
20 A. Novosselov, E. Talik and A. Pajaczkowska, *J. Alloys Compd*., 2003, **351**, 50; https://doi.org/10.1016/S0925-8388(02)01064-2.
21 D. F. Mullica, H. O. Perkins, C. K. C. Lok and V. Young, *J. Electron Spectrosc. Relat. Phenom.*, 1993, **61**, 337; https://doi.org/10.1016/0368-2048(93)80024-G.
22 J. Choisnet, N. Abadzhieva, P. Stefanov, D. Klissurski, J. M. Bassat, V. Rives and L. Minchev, *J. Chem. Soc., Faraday Trans*., 1994, **90**, 1987; https://doi.org/10.1039/FT9949001987.
23 V. Bondarenka, S. Grebinskij, V. Lisauskas, S. Mickevičius, K. Šliužiene, H. Tvardauskas and B. Vengalis, *Lith. J. Phys*., 2006, **46**, 95; https://doi.org/10.3952/lithjphys.46114.

Received: 19th August 2024; Com. 24/7599